16th World Conference on Earthquake Engineering, 16WCEE 2017

Santiago Chile, January 9th to 13th 2017

Paper N° 877 (Abstract ID)

Registration Code: S-R1460549049

ACCURACY OF MODAL COMBINATION METHODS IN SEISMIC DESIGN OF BARREL VAULT CYLINDRICAL ROOF SHELLS

S. Ostovari Dailamani [(1)], J. G.A. Croll[(2)]

[(1)] *Emeritus Professor of Civil Engineering, University College London (UCL), j.croll@ucl.ac.uk*
[(2)] *Senior Lecturer, University of Greenwich, os36@gre.ac.uk*

Abstract

The design of a structure using modal analysis is usually based on finding the maximum responses using one of the two combination methods of square-root-of -sum-of-squares (SRSS) and complete quadratic combination (CQC). It is generally accepted that the predicted approximate responses would be conservative and accurate enough for practical structural design analysis. However, in this paper it is shown that for barrel vault cylindrical roof shells the modal combination methods may not result in conservative results. In this paper a semi-analytical method, which has been previously verified using a finite element modelling, is used to find the time history response when barrel vault cylindrical shells are subject to synchronous vertical motions from typical earthquake records. The analytical method adopts an explicit solution based upon the Love-Timoshenko strain-displacement relationships and employs a Lagrangian approach to the derivation of the equations of motion. The investigation on the accuracy of modal combination methods using the two methods of square-root-of-sum-of-squares (SRSS) and complete quadratic combination (CQC) shows that both methods estimate the maximum displacement and axial membrane stresses within the practically acceptable percentage of error. However, the stress resultants other than the axial membrane stress cannot be accurately estimated using these modal combination methods and they do not always provide conservative results. It is concluded that performing a modal combination methods could lead to serious underestimation of responses for large roof shells subjected to earthquake loading.

Keywords: Roof shells; modal combination methods; seismic design; higher modes; earthquake loading

1. Introduction

The prevalence of very efficient and robust shell structures in nature has been a source of inspiration for many architects and engineers. The advancement of new optimization techniques and low mass-to-stiffness ratio of shell structures, their smooth curves and visual appeal has once again attracted engineers to explore different options of using shell structures. Their potential if designed properly to resist extreme loadings such as earthquake and hurricane has been demonstrated in recent years [1], [2].

It is, however, surprising to see so little research has been performed on the behaviour of roof shells under earthquake loading. In 1995, Kobe, a modern city was struck by M = 7.2 earthquake that caused serious and widespread damages to buildings, and infrastructure. However, shell and space frames of gymnasiums and school were not seriously affected and could serve as shelters for those who lost their homes. In an attempt to assess the maximum responses and check the efficiency of roof shells, Kuneida in 1997 investigated the response of cylindrical roofs subjected to Kobe earthquake conditions [3]. He mentioned that there was no seismic code available for the design of space structures that were built in Japan. Hence, those space structures that were built did not always follow the seismic code for buildings. Kuneida derived the maximum responses of cylindrical roof shells and domes with different geometries and material properties. However, in order to reduce the computing time he modelled them as a continuous shell. The results of the investigation showed the stresses in cylindrical shells became very large especially for in-plane shear stresses when subjected to the horizontal component of the earthquake. Other stresses were also significant for both horizontal and vertical earthquakes. Nonetheless despite the very large stresses induced in the shell modelled by

Kuneida the cylindrical roof shell in the area of earthquake were not seriously damaged. The stress responses of the domes were much less than the cylindrical shell. However, domes were subjected to an earthquake with the maximum acceleration much less than Kobe earthquake, so it was not possible to compare the level of stresses in domes with the cylindrical shells. Although Kuneida did not implement any modal combination rule to estimate the maximum responses but he suggested that the square root of the sum of squares (SRSS) estimation of the maximum response might not be valid for roof shell. The reason would be because of the closeness of natural frequencies in shells. Unfortunately as the geometry and material properties were not reported in his paper it was not possible to undertake comparative studies with Kuneida's reported results.

In 2003 Shizhao et al [4] performed a numerical study on the free vibration properties and dynamic response of single layer latticed cylindrical shell with pin joint supports to horizontal and vertical component of earthquake. They modelled latticed shell as space frame with the rigid connections between joints and did not use the equivalent shell section. They mentioned the seismic design code for latticed shell is not available in China, suggesting that it is due to the complex behaviour of this kind of structure. Based on their opinion, understanding the behaviour of latticed shell demands a huge calculation and research effort. They suggested that the complete quadratic combination (CQC) method cannot be used in such complicated structures and time history analysis (THA) method requires a lot of computing time and skilful engineers. However, they have not presented any result indicating that CQC method gives wrong estimation of results.

The result of a more recent paper shows that a response spectrum analysis, based on the current practice, where the peak modal responses are combined without including their peak factor contribution, can lead to biased estimate of the peak responses when more than one well separated modal frequencies make significant contribution to the total response [5]. Menun [5] believes there is not enough literature available about the impact of ignoring the peak factor in the response spectrum analysis.

Current modal combinations methods derive the total response based on combining the peak modal responses without including their peak factors. These peak factors are essentially the modal participation factors that are discussed for cylindrical roof shells having closely separated natural frequency in the present paper.

The present paper addresses the reliability of modal combination rules for estimating the critical dynamic response conditions for roof shells. In particular, two modal combination rules, SRSS and CQC methods are considered.

2. Analytical modelling

An analytical model is developed for a thin, open cylindrical shell, of radius of curvature R, longitudinal length $L_x = L$, thickness h, and opening angle ϕ as shown in Fig.1(a). Material is taken to be linearly elastic, and the damping ratio is taken to be constant in all modes. The analytical method is developed based on a membrane idealization of the primary equilibrium state. It adopts an explicit solution using Love-Timoshenko strain-displacement relationships and employs a Lagrangian approach to the derivation of the equations of motion. In deriving the analytical solutions based upon the above mentioned equations an exact solution for the natural vibration modes for a shell having simple support boundaries, may be taken in the form of double trigonometric series Eq. (1)

$$u(x,y,t) = \sum_i \sum_j u_{ij}(x,y) q_{ij}(t);\ v(x,y,t) = \sum_i \sum_j v_{ij}(x,y) q_{ij}(t);$$
$$w(x,y,t) = \sum_i \sum_j w_{ij}(x,y) q_{ij}(t) \quad (1)$$

where

$$u_{ij}(x,y) = \bar{u}_{ij} \cos\frac{j\pi x}{L} \sin\frac{i\pi y}{R\phi};\ v_{ij}(x,y) = \bar{v}_{ij} \sin\frac{j\pi x}{L} \cos\frac{i\pi y}{R\phi};\ w_{ij}(x,y) = \bar{w}_{ij} \sin\frac{j\pi x}{L} \sin\frac{i\pi y}{R\phi} \quad (2)$$

Each mode of this series satisfies the conditions of simple support boundaries, namely

$$v = w = 0,\ N_x = M_x = 0 \text{ at } x = 0, L \text{ and } u = w = 0,\ N_y = M_y = 0 \text{ at } y = 0, R\phi \quad (3)$$

In the modal forms of Eq. (1), (i,j) represent the number of half waves in the circumferential and longitudinal directions, respectively and $\bar{u}_{ij}$, $\bar{v}_{ij}$, and $\bar{w}_{ij}$ are the normalized coefficient determined by solving the eigenvalue problem.

Finally, for a set of cylindrical roof shells having different geometries, when subjected to the vertical motions of an earthquake will provide the basis for an assessment of the accuracy of modal combination rules in assessing the displacement, and stress responses.

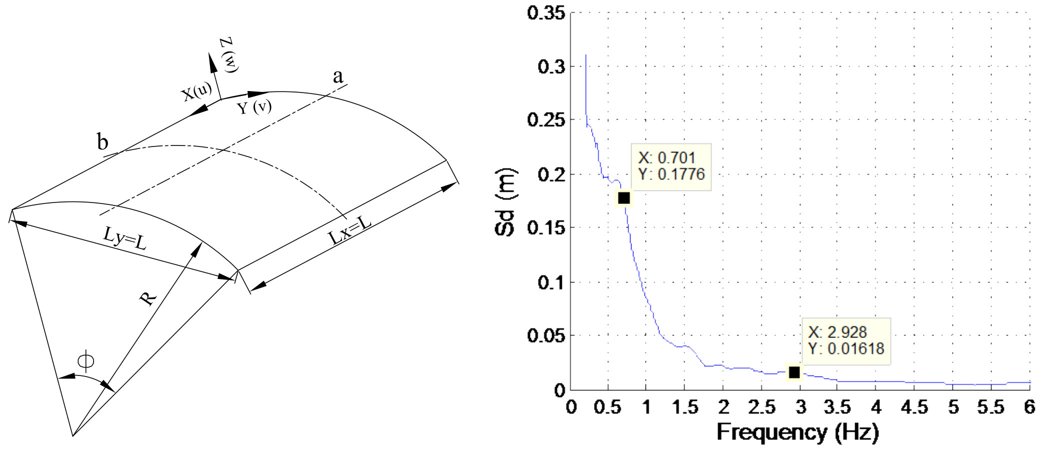

Fig. 1 – (a) Geometry of shell (b) Displacement response spectrum of Landers earthquake

2.1 Relationship between Modal Participation Factor (MPF), earthquake response spectrum and maximum response

As we know the natural frequencies and responses of a shell changed due to inclusion of typical levels of pre-loading or changes in the geometry. Therefore, it would be helpful to find simple relationships between the response spectrum of the earthquake and the observed changes in the maximum response of shell due to the changes in pre-loading or geometry of the shell. These relationships would help designers to find the maximum responses without the need to go through extensive THA. This a basis to

To address this need a study is performed, which attempts to relate the displacement response spectrum of the Landers earthquake (Fig.1(b)) to the changes in frequency due to taking into account self-weight and increasing pre-loading (Fig.2(a)), making use of the MPF of each mode (Fig.2(b)). MPF is obtained by dividing the modal force, P_{ij} by the modal mass M_{ij} as presented in Eq. (4)

$$MPF = \frac{P_{ij}\,(t)}{M_{ij}} = \frac{4(-1+\cos j\pi)(\bar{w}i\pi-\bar{v}\phi)}{j\pi(i\pi-\phi)(i\pi+\phi)}\cos\frac{\phi}{2} \qquad (4)$$

This effectively shows the inertial participation of each mode. Using MPF, the modes with higher contributions to the response would be identified. The maximum response of each mode can then be found by multiplying the values of the MPF of each selected mode by the response spectrum of the earthquake (Fig.1(b)) at the corresponding natural frequencies of the shell in that mode (Fig.2(a)).

For example, the frequency of mode (1,1) when the effect of pre-loading is neglected has the highest MPF equal to 1.4 (Fig.2(b)). The natural frequency of this mode is equal to 2.928 Hz (Fig.2(a)), for which the corresponding displacement response spectrum of earthquake, $\mathrm{S_d}$, is equal to 0.01618 m (Fig.2). Looking at the results from the THA, which represent the maximum displacement of the shell along center line bb (Fig.1(a)), it is noticed that the maximum response of mode (1,1) is equal to 0.02262 m. This value is exactly equal to the result of multiplying the value of MPF=1.4 by the value of $\mathrm{S_d} = 0.01618$ at mode (i,j)=(1,1).

Despite the increase in the levels of pre-loading and the consequent 11 % decrease in natural frequency as a result of including self-weight and the addition of self-weight plus 1500 N/m2, which reduces the natural frequency in mode (1,1) from f=2.928 Hz to f=2.637 Hz (Fig.2(a)), it is noticed that displacement response from the THA of mode (i,j)=(1,1) remains effectively constant. Using Fig.1(b) shows that the displacement response spectrum for this earthquake in the range of frequency between f=2.928 Hz and f=2.637 Hz remains constant. This explains the insignificant changes in displacement response of this mode using the THA. It should be noted that MPF of Eq. (1) should change for different levels of pre-loadings due to the changes in $\overline{w}$ and $\overline{v}$. But as the changes in $\overline{w}$ and $\overline{v}$ are insignificant, the MPF in Fig.2(b) remains constant for all levels of pre-loading.

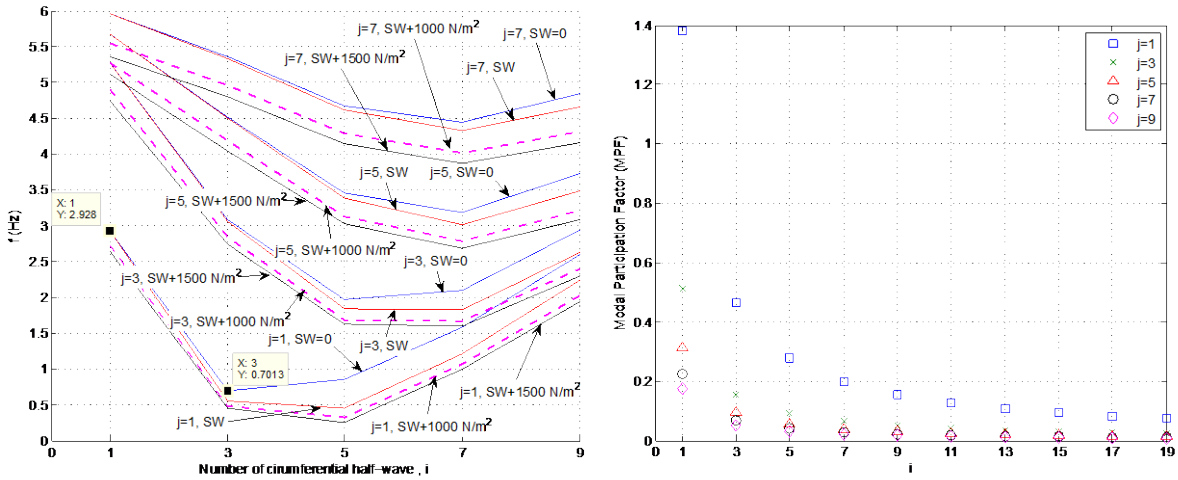

(a) Changes in natural frequency (b) Modal Participation Factor (MPF)

Fig. 2 – Active modes in response and modal participation factor for a shell with $L_y/L_x = 1$, B = $1.5 \times 10^{-6}\ s^2$

Unlike modes (1,1), The results from the modal time history analysis show that mode (5,1) displays quite considerable variations as the pre-loading increases. It shows maximum displacement of modes (5,1) equal to 0.032 m when the pre-loading is neglected. It increases to 0.055 m when including self-weight, then increases to 0.065 m corresponding to self-weight plus 1000 N/m2 additional loading, and finally reaches to 0.069 m for self-weight plus 1500 N/m2 additional loading.

The corresponding frequencies for these four cases of loading in are equal to 0.8562 Hz, 0.4498 Hz, 0.3224 Hz, and 0.253 Hz, respectively as shown in Fig.2(a).

Unlike mode (1,1), the earthquake displacement response spectra corresponding to these frequencies show significant variation in Fig.1(b). It changes from 0.1176 m, to 0.1967 m, then, 0.2326 m, and finally 0.2443 m corresponding to the aforementioned changes in frequency, respectively. This corresponds to 107 % increase in response of mode (5,1) due to inclusion of self-weight and 1500 N/m^2 additional loading.

The maximum displacement spectrum for mode (5,1) is then derived by multiplying MPF=0.28 by S_d, which is equal to 0.0329 m, 0.0551 m, 0.0651 m, and 0.0684 m, respectively. Comparing these results of 0.0329 m, 0.0551 m, 0.0651 m, 0.0684 m with the maximum displacements of 0.032 m, 0.055 m, 0.065 m, 0.069 m corresponding with mode (5,1), which are derived based on complete THA shows that they are effectively identical for practical purposes.

It is concluded that the reason for the considerable variation of displacement of mode (5,1) is because the resulting frequencies fall into a part of the earthquake displacement response spectrum, for which there is a significant variation in S_d. It should be noted that the significant decrease in frequencies are the result of the pre-loads representing a significant proportion of the critical buckling loads in this mode. These frequency changes become significantly effective as a result of the frequencies being at the sensitive area of the response spectrum.

Stresses can also be derived in a similar way to displacements. After finding the modal displacement, stresses would be derived by replacing them into Eq. (5) Maximum stresses are governed by multiplying the values of MPF of the selected modes by displacement response spectrum of the earthquake at the corresponding natural frequencies of the shell in that mode, and finally multiplying by stress factor given by the equation of stresses (Eq. (5)).

$$N_x = \frac{Eh}{1-v^2}\left(-\bar{u}_{ij}\,\frac{j\pi}{l} - v\frac{i\pi}{R\phi}\bar{v}_{ij} + \frac{v}{R}\;\bar{w}_{ij}\right)\;\sin\frac{j\pi x}{l}\sin\frac{i\pi y}{R\phi} \qquad (5)$$

As the distributions of responses are not the concern of this present study the double trigonometric series in Eq. (5) is not taken into account. In order to verify this method for stress, using Eq. (5) the values of $N_x = \frac{Eh}{1-v^2}\left(-\bar{u}_{ij}\,\frac{j\pi}{l} - v\frac{i\pi}{R\phi}\bar{v}_{ij} + \frac{v}{R}\;\bar{w}_{ij}\right)$ are plotted in Fig.3 for each of the modes i=1, 3, …, 19, and j=1,3,5. For each value of i and j this factor is then multiplied by the MPF in Fig.2(b) and the displacement response spectrum corresponding to each frequency in Fig. 1(b). The results of this multiplication are shown in Fig.3. Comparing the maximum N_x derived using this simplified method in Fig.3 and the maximum modal stress found using the THA shows that they are again basically the same. For example, the maximum value of stress resultant, N_x, at mode (1,1) using the THA is equal to $5.096 \times 10^5 N/m$. Within current accuracy this is the same as in Fig.3(b), which arises from the multiplication of the MPF=1.4 by the value of S_d=0.01616 m for mode (1,1) by the value of $N_x = 2.282\ \times 10^7 N/m^2$in Fig.3; the result would be equal to $1.4 \times 0.01616 \times 2.282 \times 10^7 = 5.096 \times 10^6 N/m$. Comparing the maximum values of the rest of the using the THA with the results in Fig.3 confirms that they too are effectively the same.

Using this method, a graph similar to the displacement response spectrum of earthquake (Fig.1(b)) can be plotted for different stress resultant. However, it should be noted that unlike the displacement response spectrum (Fig.2), which is entirely dependent upon the earthquake, the stress response spectrum is also dependent on the formulation of stress itself, which in turn is dependent to the geometry of shell. The stress response can then be derived by multiplication of the stress response spectrum by MPF. However, when stress responses are plotted in terms of frequencies as in Fig.4 it aids visualization of what range of frequencies are more important in the various membrane and bending stress resultants. It is also useful to find the maximum total stress resultant response using these maximum responses, which will be discussed in the next section.

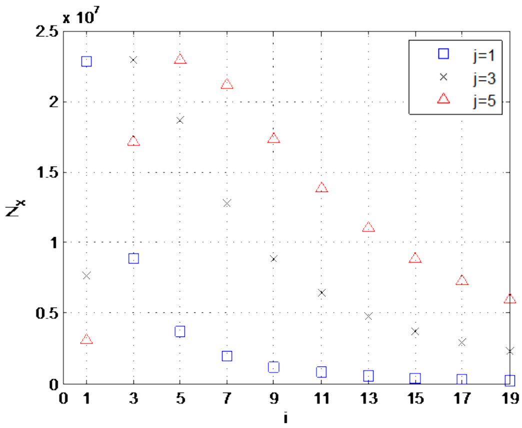

(a)

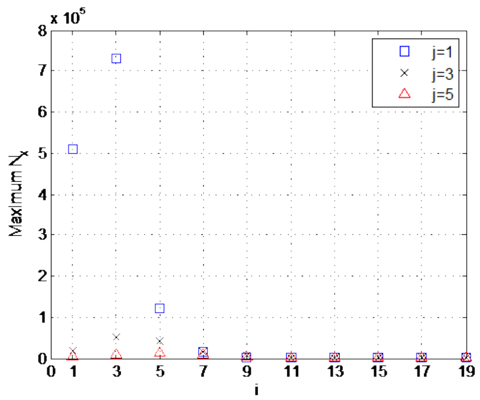

(b)

Fig. 3 – (a) : $N_x = \frac{Eh}{1-v^2}\left(-\bar{u}_{ij}\,\frac{j\pi}{l} - v\frac{i\pi}{R\phi}\bar{v}_{ij} + \frac{v}{R}\;\bar{w}_{ij}\right)$ based on Eq. (5) (b) Maximum modal N_x found by multiplying $N_x = \frac{Eh}{1-v^2}\left(-\bar{u}_{ij}\,\frac{j\pi}{l} - v\frac{i\pi}{R\phi}\bar{v}_{ij} + \frac{v}{R}\;\bar{w}_{ij}\right)$by the MPF in Fig 3(b) and the Landers earthquake displacement response spectrum in Fig 2 for a shell having $L_y/L_x = 1$, and $B = 1.5\ \times 10^{-6} s^2$

As the maximum total responses are important in design, the only aspect needed to complete the discussion is to relate the maximum modal responses to the maximum total response of shell. For ordinary frame buildings this can normally be achieved using the modal combination rule. Next section deals with the modal combination rules, and focuses on two methods for investigating whether these methods give accurate approximation of the maximum responses for shells.

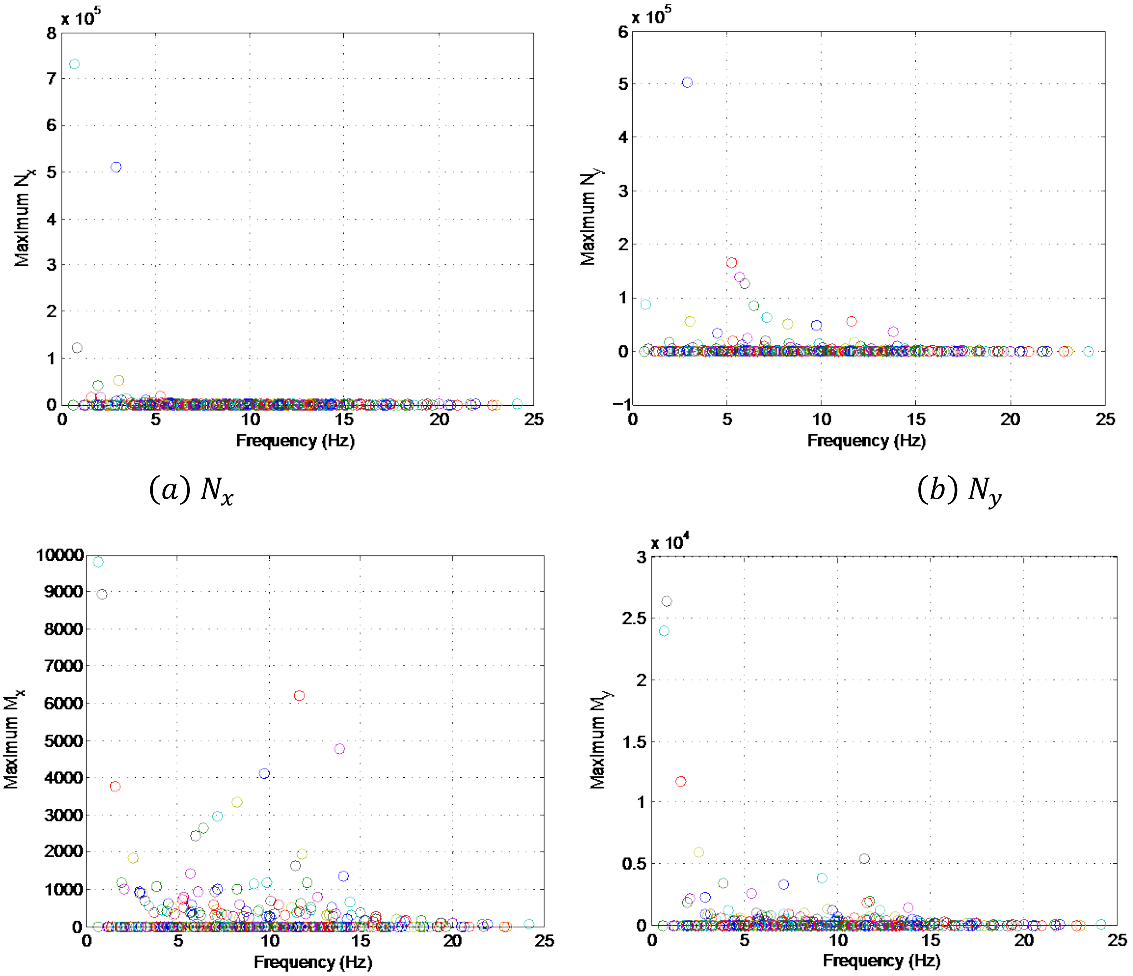

$(a)\ N_x$ $(b)\ N_y$

$(c)\ M_x$ (d) M_y

Fig. 4 – Membrane and bending stress modal contribution for a shell having $L_y/L_x = 1$, and $B = 1.5\ \times 10^{-6}s^2$ (ignoring self-weight)

2.2 Modal combination methods

In the previous section the relationships between the modal maximum response, natural frequencies of shell, and displacement and stress response spectrum of an earthquake were developed. Using these relationships makes it easy to find the maximum responses such as displacements and stress resultants in each mode without the need to go through the complete time history modal analysis.

As structural design is usually based on the peak total response values, the discussion would not be complete until the maximum modal responses could be related to the maximum total responses of the shell. This can be achieved using the modal combination methods.

Chopra [6] has outlined several methods for combining modes, while mentioning that none of these methods give exact results as the governing results are not identical to the total response using the complete THA. The reason that the responses using one or other modal combination methods are not exact, is because the modal responses reach their peak values at a different instant in time and the total maximum responses attains its peak at yet another instant in time. However, it is considered that the predicted approximate responses would be accurate enough for practical structural design analysis.

In this section, two methods of modal combination will be discussed with their predictions compared with the known maximum total responses. The response of the shell using the THA, where the effects of pre-loading are not taken into account, will be examined for each of these methods. A total of 19 by 19 half-waves in both circumferential and axial directions has been included in the THA.

The reason for not showing all contributing modes in the previous section was that the convergence of the results for total response was not the primary concern. For the sake of clarity of the plots, the contributions of modes with low responses were consequently neglected.

Multiplication of S_d by Eq. (2) is one of the methods to find the maximum response of each mode over the time history of the earthquake. The maximum modal response can then be used for estimating the maximum total response using one of the modes combining method.

The maximum response of each mode can also be derived by multiplying MPF by S_d. It is worthy to mention that this form of superposition is meant to take account of the fact that the maximum response in each mode occur at different instants of time, but at specific spatial locations on the shell surface. However another study is performed and will be presented later in this section, which examines the validity of modal combination methods when they are found regardless of the time of occurrence and its location over the surface of the shell.

The first method that will be presented here is the Square Root of the Sum of Squares (SRSS), first suggested by E. Rosenblueth as part of his PhD thesis [7], so that

$$r \approx \left(\sum_{n=1}^{N} r_n^2\right)^{0.5} \qquad (6)$$

Where r_n the peak response in each mode n, and r is the maximum value of the estimated total response. In order to check the validity of this method for shells, the maximum response of each mode regardless of time are presented in Table 1 for the shell having the natural frequency and MPF as in Fig.2.

Table 1 –Maximum modal displacement for a shell having $L_y/L_x = 1$, and $B = 1.5 \times 10^{-6} s^2$as discussed in Fig.2 (a),(b).

(i,j)	(3,1)	(5,1)	(1,1)	(7,1)	(9,1)	(5,3)	(3,3)	(1,3)	(1,5)	(1,7)	(7,3)
Max-Disp (cm)	0.082	0.033	0.022	0.008	0.002	0.002	0.002	0.002	0.001	0.001	0.001

Using the SRSS method, the maximum total displacement would be 0.0914 m. By comparing the governing maximum response using the SRSS method against the total maximum response found from the THA of 0.0953 m, it will be noticed that there is a 4.2% error as can be seen in Table 2 for a shell with $L_y/L_x = 1$, and $B = 1.5 \times 10^{-6} s^2$.

As Chopra explained [6] the SRSS method gives practically accurate estimates of the responses in structures with well-separated frequencies such as frames. However, for systems with closely spaced natural frequencies such as piping and multi-storey buildings with unsymmetrical plan it will not provides accurate responses. As the shell is a system with closely spaced natural frequencies, this method may not always be used reliably.

The next method for modal combination is the Complete Quadratic Combination (CQC), which is applicable to a wider range of structures and is suggested to provide accurate results for structures with closely-spaced frequencies [6]. The maximum total response using CQC method is derived using

$$r_o \approx (\sum_{i=1}^{N}\sum_{n=1}^{N}\rho_{in} r_{io} r_{no})^{0.5} \tag{7}$$

Where r_{io} , and r_{no} are the peak responses in the i[th] and n[th] modes and ρ_{in} is the correlation coefficient for these two modes. ρ_{in} varies between 0 and 1 and it is equal to 1 when i=n. Eq. (8) can be rewritten as the sum of the SRSS plus the additional term as

$$r_o \approx (\sum_{n=1}^{N} r_{no}^2 + \underbrace{\sum_{i=1}^{N}\sum_{n=1}^{N}}_{i\neq n}\rho_{in} r_{io} r_{no})^{0.5} \tag{8}$$

The first term in Eq. (8) is identical to SRSS and is positive, however the second term may be positive or negative. Thus the result using CQC method could be either less or more than the governing results using SRSS method. There are several definition for the correlation coefficient proposed by researchers. However, in this section the Rosenblueth-Elorduy definition that is given by Newmark and Rosenblueth in the textbook Fundamentals of Earthquake Engineering [7] is used for a constant value of damping ratio, ζ, in all modes as

$$\rho_{in} = \frac{\zeta^2(1+\beta_{in})^2}{(1-\beta_{in})^2 + 4\zeta^2\beta_{in}} \tag{6.5}$$

where $\beta_{in} = \frac{w_i}{w_n}$ is the ratio of frequencies in modes i and n.

The maximum displacement prediction using the CQC method for the shell in Fig.2 is equal to 0.0974 m, which as can be seen in Table 2 for the shell with $L_y/L_x = 1$, and $B = 1.5 \times 10^{-6} s^2$ has just a 2.2% error as compared with the maximum displacement of 0.0953 m using the time history analysis. This is lower than the 4.09% error using the SRSS method as shown in Table 2.

As mentioned earlier two methods are chosen in this study to find the maximum responses of the shell. First method finds the maximum responses of the shell for every points over the surface of the shell but only regardless of the time. The second method finds the maximum responses of the shell regardless of where and when they occur.

Table 2 provides the summary of the maximum displacement and stress responses for three cases of shell using the complete modal time history analysis (THA) method and compares with the responses using the SRSS, CQC at the same location where the maximum response using the time history analysis occurs.

As mentioned, the peak responses using either SRSS or CQC method are governed by finding the maximum modal response regardless of the time of occurrence but taking into account their location over the surface of the shell. In other words it finds the maximum modal response at each point over the surface of the shell and combines them accordance with one of the combination methods (SRSS and CQC). In this way a maximum response would be attained for every point over the surface of the shell.

Table 2 – Comparison of the results between modal time history analysis, CQC, and SRSS for a total number of 19 axial and circumferential half waves including effect of location

	L_y/L_x	B	THA	SRSS	CQC	% error SRSS	% error SRSS
W (m)	1	1	0.0663	0.0593	0.0585	10.56	11.76
	1	1.5	0.0953	0.0914	0.0974	4.02	2.2
	2	1.5	0.0183	0.0161	0.015	12.02	18.03
$N_x(N.m^{-1}) \times 10^6$	1	1	1.0494	0.9820	0.9935	6.43	5.33
	1	1.5	0.8741	0.9016	0.9419	3.16	7.77
	2	1.5	0.2607	0.2943	0.2936	12.91	12.63
$N_y(N.m^{-1}) \times 10^6$	1	1	0.7897	0.4707	0.6623	40.39	16.14
	1	1.5	0.5737	0.5918	0.5825	3.15	1.54
	2	1.5	0.5835	0.4294	0.4170	26.41	28.54
$N_{xy}(N.m^{-1}) \times 10^6$	1	1	0.9348	0.6042	0.6745	35.36	27.85
	1	1.5	0.6176	0.5902	0.6374	4.43	3.21
	2	1.5	0.4131	0.3253	0.3482	21.25	15.71
$M_x(N.m) \times 10^4$	1	1	2.5194	1.6260	1.9647	35.46	22.02
	1	1.5	1.7751	1.3679	1.3648	22.94	23.12
	2	1.5	1.5797	1.7111	1.4289	8.32	9.55
$M_y(N.m) \times 10^5$	1	1	0.6663	0.4302	0.4619	35.43	30.67
	1	1.5	0.4483	0.3444	0.163	23.16	29.44
	2	1.5	0.1698	0.1560	0.1575	8.18	7.26
$M_{xy}(N.m) \times 10^4$	1	1	1.8188	0.9580	1.2093	47.33	33.51
	1	1.5	1.1770	0.7249	0.8038	38.42	31.71
	2	1.5	0.8243	0.4833	0.6165	41.36	25.20

The modal combination methods are also used to find the maximum stress resultants. The maximum modal stress resultants shown in Table 2 for three cases of shells, are derived using the maximum modal stresses governed by the method described in section 2.1. The maximum stress responses are derived over the time history of earthquake and at each point over the surface of the shell. Same as displacements, the maximum stresses and their location are found using the THA method. The maximum stresses are then compared with the maximum stresses using the SRSS and CQC method at the location where the maximum stress resultants are found using THA method; these are reported in Table 2.

In Table 2 the error in SRSS and CQC method are expressed as a percentage of the maximum result derived using the time history modal analysis. It is noticed that the peak response using approximate methods can be either lower or higher than the THA value. The error is different for each of the membrane and bending stress resultants; for example for the case of shell with $L_y/L_x = 1$ and $B = 1 \times 10^{-6} s^2$, the error in Nx is less than the error in Ny, My, and Mx (Table 2). The reason that the error is smallest in Nx is that the modes with higher frequencies do not contribute to the total response. However, modes with higher frequencies contribute to the total response more significantly in Ny, My, and Mx; so the error of using the combination methods are higher in these responses. The error in displacement for this case of shell ($L_y/L_x = 1$ and $B = 1 \times 10^{-6} s^2$) is also small; again because the modes participating in the total responses have low frequencies.

The SRSS and CQC methods do not give the same estimates of peak stress responses. Analysis on three cases of shells in Table 2 shows that the CQC method does not always produce lower percentage errors than the SRSS method as is often accepted by many researchers.

However, another method is proposed in this research, which can be named as second approach for finding the maximum response. This method also uses the method of section 2.1 in finding the maximum responses not only over the duration of earthquake, but also over the surface of the shell. The displacement and the stress resultants using this method are shown in Table 3.

As can be seen, the percentage of error for CQC and SRSS method for shells using this second method can be either higher or lower than the first method. However, the maximum displacement (W), N_{xy} and M_{xy} response in Table 2 seems to be the same as in Table 3.

As can be seen by comparing Tables 2 and 3 some stress resultants have changed significantly as a result of taking into account the location over the surface of the shell in finding the modal peak responses; such as the error corresponding to CQC method in M_x for a shell with $L_y/L_x = 1$ and $B = 1 \times 10^{-6} s^2$, that has reduced from 103.87 % to 9.55 % in Table 3. It is noted that using these two methods does not change the governing peak displacement response using SRSS method.

The significant change in the result using CQC method based on the two aforementioned methods is a result of the cross-correlation coefficient being significant when the peak modal displacement responses are chosen, regardless of its location over the surface of the shell. This shows that CQC method is sensitive to the location of the peak modal responses over the surface of the shell and peak responses happening at different locations of the shell cannot simply be combined using the CQC method. In other words in CQC method, the maximum modal displacement responses that are derived regardless of the time of occurrence over the time history of earthquake but taking into account the location are more reliable. The maximum responses over the surface of the shell can then be found from the peak nodal responses.

However, finding the peak responses regardless of time and location has the advantage of reducing the calculation time significantly. As both methods give the same displacement response as of SRSS method, the latter method can be accurately used for SRSS method.

For the three cases of shells in Table 2 the maximum error using SRSS remain less than 12.02% and for CQC less than 18.03% for displacement. However, for stress resultants such as N_y the errors are respectively less than 40.39% and 28.54%. The error for axial stress, N_x, which has only the contribution from modes with low frequencies also remain less than 12.91% and 12.63% respectively using SRSS and CQC method. It can be concluded that the modal combination method can only give practically acceptable errors for displacement and axial membrane stress resultant. However, the stress resultants other than N_x cannot be estimated accurately using the modal combination methods.

Table 3 – Comparison of the results between modal time history analysis, CQC, and SRSS for a total number of 19 axial and circumferential half waves neglecting effect of location

	L_y/L_x	B	THA	SRSS	CQC	% error SRSS	% error CQC
W (m)	1	1	0.0663	0.0593	0.0638	10.56	3.77
	1	1.5	0.0952	0.0914	0.864	4.09	9.34
	2	1.5	0.0183	0.0201	0.02	9.84	9.29
$N_x(N.m^{-1}) \times 10^6$	1	1	1.0494	1.074	1.135	2.34	8.16
	1	1.5	0.8741	0.9016	0.9121	3.15	4.35
	2	1.5	0.2607	0.2943	0.2813	12.89	7.90
$N_y(N.m^{-1}) \times 10^6$	1	1	0.7897	0.7552	1.0775	4.37	36.44
	1	1.5	0.5737	0.5918	0.7737	3.15	34.86
	2	1.5	0.5835	0.6646	0.8167	13.90	39.97
$N_{xy}(N.m^{-1}) \times 10^6$	1	1	0.9348	0.6042	0.6745	35.37	27.85
	1	1.5	0.6176	0.5902	0.6374	4.44	3.21
	2	1.5	0.4131	0.3253	0.3482	21.25	15.71
$M_x(N.m) \times 10^4$	1	1	2.5194	2.6736	3.9476	6.12	56.69
	1	1.5	1.7751	1.8441	2.9145	3.89	64.19
	2	1.5	1.5797	1.9659	3.2205	24.74	103.87
$M_y(N.m) \times 10^5$	1	1	0.6663	0.5267	0.6015	20.95	9.73
	1	1.5	0.4483	0.3951	0.412	11.87	8.10
	2	1.5	0.1698	0.1807	0.2509	8.19	47.76
$M_{xy}(N.m) \times 10^4$	1	1	1.8188	0.9580	1.2093	47.33	33.51
	1	1.5	1.1770	0.7249	0.8038	38.41	31.71
	2	1.5	0.8906	0.4386	0.6233	50.75	30.31

The results of this section show that the percentage of error is different for each of the membrane, bending stress resultant, and displacement responses. The results are also dependent on the material properties and geometry of the shell, which determine the natural frequencies of the shell. Using the combination methods for finding the displacements are more reliable than for stresses; this can be seen in Table 2.

3. Conclusions

A literature review was first performed to find the gaps in understanding of the dynamic analysis of roof shells. The equations of motion for a complete cylindrical shell were derived based on the energy formulation was used to find the equation of motion in roof shells. The method is based on the stationary of total potential energy for providing the equilibrium in the structure. This study led to an investigation to find a simple relationship between the modal participation factor, earthquake response spectrum and maximum displacement and stress resultant responses of the shells without going through the extensive time consuming time history analysis. The aim was to examine the accuracy of the modal contribution methods to find the maximum responses of a shell. These methods are conveniently used for frame buildings and result in practically accurate results.

Using the equation of the modal participation factor helps to identify the modes with higher contributions. The maximum modal displacements were then found by multiplying the mode participation factor (MPF) by the displacement response spectrum of the earthquake corresponding to the natural frequency of the shell in that mode. This showed that the mode having the highest MPF does not necessarily have the highest contribution to the total response. This is because the contribution of the mode to the total response also depends on the response spectrum of the earthquake at the natural frequency of the shell corresponding to that mode.

The maximum stress responses were also derived by multiplying the maximum displacement response by the stress factor given by the equations of stress resultants. These were the same as the maximum modal responses using the time history analysis. The investigation on the accuracy of modal combination methods using the two methods of square-root-of-sum-of-squares (SRSS) and complete quadratic combination (CQC) showed that both methods estimated the maximum displacement and axial membrane stresses within the practically acceptable percentage of error; although the percentages of errors were different for various geometries of shells. However, the stress resultants other than axial membrane stress cannot be accurately estimated using either of these modal combination methods.

4. References

[1] South A, Zweifel C (2014): Disaster Survivability of Thin-Shell Concrete Dome Structures: Experience and Practice. *IASS-SLTE 2014 Symposium "Shells, Membranes and Spatial Structures: Footprints"*. Brasilia, Brazil.

[2] South A, Zweifel C (2014): Concrete Dome Structures and Extreme Wind Loads: The Design of Community Shelters. *IASS-SLTE 2014 Symposium "Shells, Membranes and Spatial Structures: Footprints"*. Brasilia, Brazil.

[3] Kuneida H (1997): Earthquake response of roof shells. *International Journal of Space Structures*, **12**, 149-160.

[4] Shen S, Xing J, Fan F (2003): Dynamic behavior of single-layer latticed cylindrical shells subjected to seismic loading. *Earthquake Engineering & Engineering Vibration*, **2** (2), 269-279.

[5] Menun C, Reyes JC, Chopra AK (2015): Errors caused by peak factor assumptions in response-spectrum-based analyses. *Earthquake Engineering & Structural Dynamics*, ***44***(11), 1729-1746.

[6] Chopra AK (2014). Dynamics of structures: theory and applications to earthquake engineering. Prentice Hall, 4th Edition.

[7] Newmark NM, Rosenblueth E (1971): Fundamentals of earthquake engineering. Prentice-Hall Englewood Cliff, NJ, 1971